

Hydrodynamic simulations of laser interactions with low-density foams

T. KAPIN, M. KUCHARÍK, J. LIMPOUCH, R. LISKA

*Czech Technical University in Prague, Faculty of Nuclear Sciences and Physical Engineering, Břehová 7, 115 19 Praha 1, Czech Republic
e-mail: kapin@snehurka.fjfi.cvut.cz*

Received 1 April 2006

Low-density foam layers may be utilized in inertial fusion targets for smoothing of transverse inhomogeneities in ablation pressure. Alternatively, transparent underdense foam may serve as a dynamic phase plate for spatiotemporal smoothing of inhomogeneity patterns inside laser beams. We present here results of one- and two-dimensional fluid simulations of laser interactions with foams. For foams with submicron pores and wall thicknesses of order 10 nm, laser tunneling through overdense ionized walls is observed and laser penetration into the foam is accelerated. Qualitative comparison with recent experimental results is performed.

PACS: 52.50.Jm, 52.65.Kj

Key words: fluid simulations, foam microstructure, laser penetration

1 Introduction

Foam layers may significantly improve target design for inertial confinement fusion. The original proposal [1] is a hybrid indirect-direct scheme. It assumes conversion of the laser pulse front edge in a very thin outer high-Z foil into X-rays, that preheat thick layer of low density foam. Then inhomogeneities in the irradiation pattern are smoothed out by heat conduction in the layer of preheated foam material and symmetric implosion of the inner fuel capsule is thus achieved. Similar scheme was later studied experimentally [2], where significant growth reduction of the transverse inhomogeneities of the inner accelerated shell was observed even when the outer Au-foil was absent and laser was focussed directly on the foam layer. Even much earlier [3] directly-driven ICF targets were proposed with the outer low-density foam layer, that serves, both as efficient absorber of laser radiation, and for smoothing of transverse inhomogeneities in ablation pressure. Alternatively, preformed plasma prepared from preheated underdense (electron density in fully ionized homogenized foam material below critical) foam may serve as a dynamic phase plate for spatiotemporal smoothing of inhomogeneity patterns inside laser beams [4]. Detailed information about laser-foam interactions is needed for reliable utilization of low-density foam layers. Laser absorption, energy transfer and shock wave propagation in underdense foams has been recently studied experimentally at sub-nanosecond kJ iodine laser PALS [5, 6]. Qualitative theory[7] of laser foam interaction introduces fast homogenization stage, when empty spaces inside foam pores are filled by plasma expanding from pore walls. Then, colliding plasma flows oscillate inside the pores until they are gradually damped out by viscosity during

slow homogenization stage. Pressure of propagating shock wave may be estimated in approximation of homogeneous low density media but this model overestimates the shock wave speed significantly [8].

Simulations of laser interactions with foams are complicated by the difference between microscopic pore dimensions and macroscopic experimental scales. Foam was numerically modeled by a set of slabs with intermediate void spaces in one-dimensional (1D) simulations of laser penetration and energy transport into the foam [9]. Brickwork structure was applied in 2D simulations of homogenization of laser heated foams [10]. Our paper is devoted to 1D and 2D fluid simulations of laser penetration into underdense foams of various cell sizes and densities. Both in 1D and 2D simulations, foam is represented by set of thin slabs with intermediate void spaces. Regimes of exploding foils and ablatively accelerated foils are identified for foams with lighter and heavier slabs, respectively. Simulations are conducted for conditions of recent experiments in PALS laboratory [11].

2 One-dimensional and two-dimensional studies

One-dimensional studies are accomplished by code employing standard staggered Lagrangian one temperature hydrodynamical method with QEOS equation of state [12] accompanied by standard Spitzer-Harm heat conductivity [13] with heat flux limitation by $Q_{lim} = fkn_e v_{Te} T_e$ where n_e is the electron density, k Boltzmann constant, v_{Te} thermal velocity of electrons, T_e electron temperature and we have used the limiter $f = 0.03$. For laser absorption two models are included in 1D code. The simple absorption on the critical surface assumes that the laser penetrates till the critical surface and is absorbed on the critical surface. We estimate the laser absorption to 50 % for the first harmonics and to 75 % for the third harmonics. The detailed laser absorption model is based on stationary Maxwell equations from which stationary 1D wave equation is derived. The wave equation is solved inside each computational cell where the constant uniform plasma properties (density, ionization, temperature) are assumed and in each mesh node where the properties have a jump. The complex permittivity appearing in the wave equation depends on laser, plasma and collision frequencies. The solution of the wave equation provides the reflection and absorption coefficients on each cell interface (node). The laser intensities at the nodes are given by the reflection and absorption coefficients and the permittivity. The Lagrangian internal energy equation contains the divergence of the laser intensity as a source term which transfers energy from laser into the plasma. This approach allows to simulate interaction of laser beam with completely underdense targets.

We model the foam by series of uniform high density slabs and low density voids (due to numerical reasons we cannot set the void density to zero). The thickness of the high density slabs is much smaller than the thickness of the voids. For the first two tests we assume that the thickness of one slab with one void is $2 \mu\text{m}$. The foam with thick slabs has the slab thickness $0.02 \mu\text{m}$ and the foam with thin slabs has the slab thickness $0.01 \mu\text{m}$. The slab density is 1 g/cm^3 and the void density is

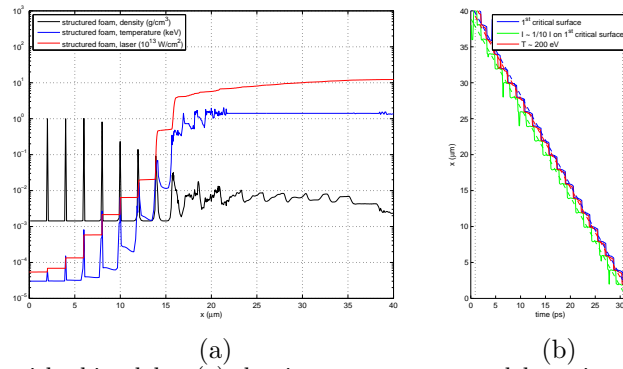


Fig. 1. Foam with thin slabs: (a) density, temperature and laser intensity profiles for structured density; (b) penetration of laser into the foam target measured by position of critical density, decrease of laser intensity and 200 eV temperature.

$1.43 \text{ mg}/\text{cm}^3$. We simulate only 20 slabs of foams with both thick and thin slabs irradiated by iodine laser of maximum intensity $3.7 \cdot 10^{14} \text{ W}/\text{cm}^2$ on the third harmonics with wavelength $0.438 \mu\text{m}$. The laser intensity increases fast from zero to the given maximum value during the first 1 ps of the simulations and then stays constant on the maximum value. The results for the foam with thin slabs is shown in Fig. 1 (a) presenting density, temperature and laser intensity at time 20 ps. The laser burns through several slabs at once in explosive regime which can be seen in the density plot as four slabs with density decreasing from about $0.7 \text{ g}/\text{cm}^3$ to the values about $10^{-2} \text{ g}/\text{cm}^3$ and in the laser intensity plot as its staircase increase over the region of these slabs. This should be compared with Fig. 2(a) presenting the same quantities for the foam with thick slabs where only one slab at time is burned by laser in ablative regime with density of only one slab being below $1 \text{ g}/\text{cm}^3$ and above $10^{-2} \text{ g}/\text{cm}^3$ and laser intensity dropping down quickly at the region of this burned slab.

From experimental measurement we can get the velocity of laser penetration into the foam target. The velocity of the laser penetration can be determined from simulation results by three methods, all of them should give similar results. The first method employs the speed of critical surface position. The second method, based on the laser intensity decrease, follows the position of the point at which the laser intensity value is 10% of the laser intensity at the critical surface. And the third method follows the position with 200 eV temperature. This temperature value has been chosen as it is the threshold temperature value of streak camera used on PALS experiments. However, this temperature based method cannot be applied on the first steps of the simulation as the whole target has lower temperature. Fig. 1(b) and Fig. 2(b) present the laser penetration for foams with thin and thick slabs respectively. The dependence of laser head position, i.e. the point up to which laser penetrates, on time is plotted by all three methods. In all the cases the overall

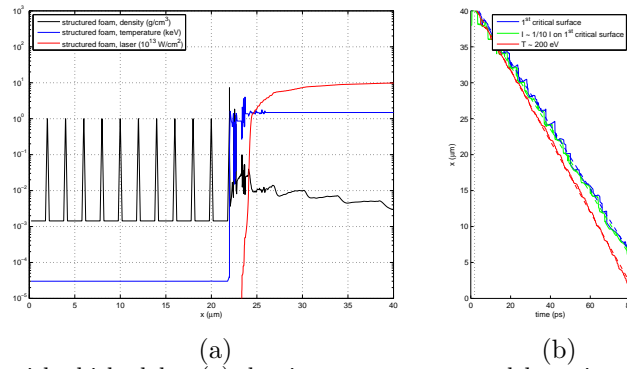


Fig. 2. Foam with thick slabs: (a) density, temperature and laser intensity profiles for structured density; (b) penetration of laser into the foam target measured by position of critical density, decrease of laser intensity and 200 eV temperature.

dependence is approximately linear as the laser intensity is constant since time 1 ps. To get the speed of penetration we interpolate the dependence of position on time into one linear line by least squares and the slope of the line gives us the penetration speed. For the foam with thin slabs the speeds obtained by all three methods are approximately the same (see Fig. 1(b)) while for the foam with thick slabs the speed obtained by critical surface and intensity decrease are approximately the same and the speed from temperature is higher (see Fig. 2(b)). This corresponds with Fig. 2(a) where one can notice that heat wave is faster than the laser intensity wave corresponding to the critical surface position.

The laser interaction with foam with thick slabs described above is simulated in 2D by our ALE code. The foam is modelled by uniform high density slabs separated by low density voids. The radius of laser spot on target is $125\ \mu\text{m}$ and laser is assumed to have Gaussian profile in space. All the remaining data are the same as

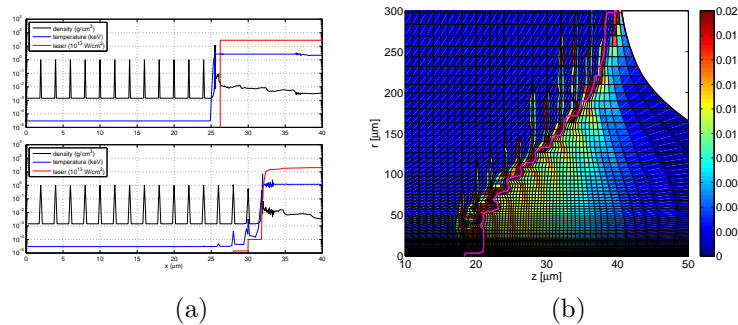


Fig. 3. Foam with thick slabs at time 20 ps: (a) 1D density, temperature and laser intensity profiles with laser absorption on critical surface (upper plot) and detailed laser absorption (lower plot); (b) density colormap of 2D simulation with critical surface.

in 1D. The laser absorption in the 2D ALE code is modeled by the simple model of absorption on the critical surface. The absorption rate for the third harmonics is estimated to 75%. Fig. 3(b) presents the density colormap of 2D simulation at time 20 ps together with critical surface at which the laser is absorbed showing that 10 slabs are burned on the z axis. For comparison in Fig. 3(a) we present corresponding 1D results with absorption on the critical surface (8 slabs are burned) in upper plot and with detailed absorption (5 slabs are burned) in the lower plot. The laser penetration is faster for absorption on critical surface than for detailed absorption. The laser penetration with absorption on critical surface in 2D is faster than in 1D probably due to higher laser intensity on z axis using 2D Gaussian profile in r while 1D simulation uses the average intensity.

3 1D simulations of TAC foam experiments

The next simulations correspond to real experiment performed at PALS. The target consists of $400\ \mu\text{m}$ thick TAC foam with mean density $9.1\ \text{mg}/\text{cm}^3$ and $2\ \mu\text{m}$ thick pores which is modeled as a set of segments with $18\ \text{nm}$ thick slabs with density $1\ \text{g}/\text{cm}^3$ and $1.982\ \mu\text{m}$ voids with density $10^{-4}\ \text{g}/\text{cm}^3$. The simulation results are influenced mainly by the mass of slabs, the results with slabs density $2\ \text{g}/\text{cm}^3$ and corresponding barrier thickness (with the same mean density) gave very similar results. The Gaussian laser pulse on the third harmonics with energy $170\ \text{J}$, with the radius of laser spot on target $300\ \mu\text{m}$ and with the full width at half maximum length $320\ \text{ps}$ approximates reasonably the experimental laser. We start the simulation $500\ \text{ps}$ before the laser maximum. In the second experiment the $380\ \mu\text{m}$ thick TAC foam target has the mean density $4.5\ \text{mg}/\text{cm}^3$ with $2\ \mu\text{m}$ thick pores which is modeled as a set of segments with $8.8\ \text{nm}$ thick slabs with density $1\ \text{g}/\text{cm}^3$ and $1.9912\ \mu\text{m}$ voids with density $10^{-4}\ \text{g}/\text{cm}^3$.

The density, temperature and laser intensity for $9.1\ \text{mg}/\text{cm}^3$ TAC foam is plotted in Fig. 4(a) which also includes results using initial uniform density (in dashed lines). The structured foam (with slabs) is burned in ablative regime. Uniform and structured results differ a lot. The laser penetrates into the uniform density target much faster than into the structured one. Apparently for foams simulations we cannot use uniform initial density as it is giving incorrect results. Fig. 4(b) and Fig. 4(c) present the laser penetration for $9.1\ \text{mg}/\text{cm}^3$ and $4.5\ \text{mg}/\text{cm}^3$ TAC foams respectively. As the temporal profile of laser is Gaussian the penetration curves are no longer close to linear. By linear interpolation on $200 - 500\ \text{ps}$ interval (laser maximum is at $500\ \text{ps}$) for $9.1\ \text{mg}/\text{cm}^3$ TAC foam and on $200 - 405\ \text{ps}$ (the whole target is burned through at $405\ \text{ps}$) for $4.5\ \text{mg}/\text{cm}^3$ TAC foam we get linear functions shown in dashed lines giving us the penetration speeds. The $4.5\ \text{mg}/\text{cm}^3$ TAC foam is burned in exploding regime much faster than the $9.1\ \text{mg}/\text{cm}^3$ TAC foam burned in ablative regime. For $9.1\ \text{mg}/\text{cm}^3$ TAC foam the penetration speed obtained by the critical surface position is $4.6 \cdot 10^7\ \text{cm}/\text{s}$, the speed by the laser intensity decrease is $4.9 \cdot 10^7\ \text{cm}/\text{s}$, while the temperature based method gives $5.4 \cdot 10^7\ \text{cm}/\text{s}$ for structured and $1.2 \cdot 10^8\ \text{cm}/\text{s}$ for uniform foam simulations. Velocity from experiment is

approximately $6 \sim 7 \cdot 10^7$ cm/s before the laser pulse reaches its maximum. Compared to this value, the structured foam results fit better than the uniform one. For 4.5 mg/cm^3 TAC foam the penetration speeds obtained all three methods are very close to $1.3 \cdot 10^8$ cm/s, while the temperature based method gives $2.2 \cdot 10^8$ cm/s for uniform foam simulations. Velocity from experiment is approximately $1.3 \cdot 10^8$ cm/s before the laser pulse reaches its maximum which corresponds reasonably well to structured simulations results.

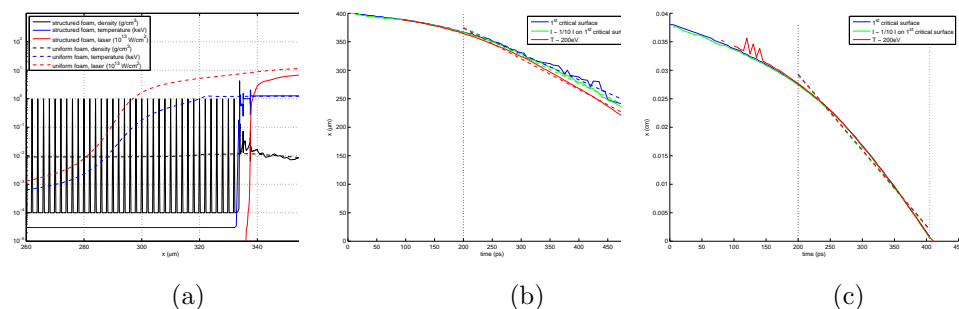


Fig. 4. (a) density, temperature and laser intensity profiles for structured density (solid lines) and uniform mean density (dashed lines) for 9.1 mg/cm^3 TAC foam at time 280 ps; (b) 9.1 mg/cm^3 TAC foam and (c) 4.5 mg/cm^3 TAC foam penetration of laser into the foam target measured by position of critical density, decrease of laser intensity and 200 eV temperature.

This research has been partly supported by the Czech Ministry of Education projects LC528 and MSM 6840770022, and the Czech Science Foundation project GACR 202/03/H162.

References

- [1] M. Desselberger, M. W. Jones, J. Edwards, *et al.*: Phys. Rev. Lett. **74** (1995) 2961.
- [2] H. Nishimura, H. Shiraga, H. Azechi *et al.*: Nuclear Fusion **40** (2000) 547.
- [3] S. Yu. Gus'kov, N. V. Zmitrenko, V. B. Rozanov: JETP **81** (1995) 296.
- [4] P. Michel, C. Labaune, H. C. Bandulet *et al.*: Phys. Rev. Lett. **92** (2004) 175001.
- [5] J. Limpouch, N. N. Demchenko *et al.*: Plasma Phys. Contrl. Fusion **46** (2004) 1831.
- [6] J. Limpouch, N. N. Demchenko *et al.*: Laser & Particle Beams **23** (2005) 321.
- [7] S. Yu. Gus'kov, V. B. Rozanov: Quantum Electron. **27** (1997) 696.
- [8] M. Kalal, J. Limpouch, E. Krousky *et al.*: Fusion Sci. Technol. **43** (2003) 275.
- [9] R. J. Mason, R. A. Kopp, H. X. Vu *et al.*: Phys. Plasmas **5** (1998) 211.
- [10] S. Yu. Gus'kov, N. N. Demchenko *et al.*: Quantum Electron. **33** (2003) 95.
- [11] J. Limpouch, N. G. Borisenko, N. N. Demchenko *et al.*: J. Phys. IV (2006) (in print).
- [12] R. M. More, K. Warren, D. Young, G. Zimmerman: Phys. Fluids **31** (1988) 3059–3078.
- [13] L. Spitzer, R. Harm. Phys. Rev. **89** (1953) 977–981.